Discover Applied Sciences

Research

Spectroscopic investigations of green synthesized zinc oxide nanoparticles (ZnO NPs): antioxidant and antibacterial activity

Ajay Kumar Tiwari[1] · Saket Jha[2] · Sharad Kumar Tripathi[3] · Rohit Shukla[4] · Ram Raseele Awasthi[5] · Abhishek Kumar Bhardwaj[6] · Abhimanyu Kumar Singh[7] · Anupam Dikshit[8]

Received: 11 November 2023 / Accepted: 20 June 2024
Published online: 24 July 2024
© The Author(s) 2024 OPEN

Abstract
In the recent decade, zinc oxide nanoparticles (ZnO NPs) have been widely explored owing to their versatile properties and prodigious demands in the drug delivery, medical, energy storage, cosmetics, and the healthcare sectors. Therefore, the current work opts for an environmentally benign method to prepare ZnO NPs. The leaf extract of *Calendula officinalis L.* acts as a reducing agent for the metal ions; therefore, in the current research, ZnO NPs were prepared via green route by using *Calendula officinalis* leaf extract. Furthermore, the ZnO NPs were analysed with different spectroscopic techniques to confirm the structure and stability of nanomaterials. The prepared ZnO NPs were characterized by XRD, FE-SEM, FT-IR and UV–Vis studies. Also, the antioxidant and antimicrobial properties of the synthesized ZnO NPs were investigated. The XRD result of synthesized ZnO NPs showed the crystalline size 28.23 nm with wurtzite hexagonal structure along with the most intense peak (101). Following preliminary confirmations of the intended ZnO NPs, both big and small agglomerated forms were observed in the FE-SEM, which is often used to determine their exterior assembly. Further, the results of Fourier transform infrared spectroscopy (FT-IR) indicated the formation of pure ZnO NPs with an absorption peak of the Zn–O bond between 4000 cm^{-1} and 500 cm^{-1} and no discernible peak in the monitoring range. The UV–Vis spectrum of the green synthesized ZnO NPs were revealed two prominent absorption peaks at 355 nm and 370 nm with energy band gap of 2.986 eV. Using the 1, 1-di phenyl-2-picrylhydrazyl (DPPH) test, the antioxidant activity of the described ZnO NPs was assessed. It demonstrated how, ZnO NPs significantly increased their antioxidant activity by scavenging 1, 1-di phenyl-2-picrylhydrazyl (DPPH) free radicals. It could be seen that synthesis of the naturally occurring plant product ZnO NPs have been acting as an alternate of chemical antioxidant. The antimicrobial analysis was also performed with the help of disk diffusion method where three multi-drug resistant human pathogens namely *Staphylococcus aureus, Klebsiella pneumoniae and E.coli* were used. The Zone of Inhibition diameter values are 35.2 mm ± 0.9, 23.6 mm ± 0.1 and 13.5 mm ± 0.1, respectively, which showed that the ZnO NPs was highly effective against *S. aureus*. Thus, the green

Ajay Kumar Tiwari and Saket Jha have contributed equally to this work.

✉ Ajay Kumar Tiwari, drajayngbv@gmail.com; ✉ Abhishek Kumar Bhardwaj, bhardwajak87@gmail.com; Saket Jha, jhasaket90@gmail.com; Sharad Kumar Tripathi, sharadtripathi92@gmail.com; Rohit Shukla, mr.rohitbplau@gmail.com; Ram Raseele Awasthi, rrawasthi1947@gmail.com; Abhimanyu Kumar Singh, abhimanyu.kr.singh@gmail.com; Anupam Dikshit, anupambplau@gmail.com | [1]Department of Physics, Nehru Gram Bharati (Deemed to be University), Prayagraj 221505, U.P., India. [2]Department of Surgery, University of Illinois at Chicago (UIC), Chicago, Illinois 60612, USA. [3]Department of Life Sciences, Arni University, Kangra, H.P. 176401, India. [4]Centre of Science and Society, Under IIDS, University of Allahabad, Prayagraj 211002, U.P., India. [5]Faculty of Engineering and Technology, Khwaja Moinuddin Chishti Language University, Lucknow 226013, U.P., India. [6]Department of Environmental Science, Amity School of Life Sciences, Amity University Madhya Pradesh, Gwalior 474 005, M.P., India. [7]Department of Physics, Shyama Prasad Mukherjee Govt. Degree College, University of Allahabad, Prayagraj 211013, U.P., India. [8]Biological Product Laboratory, Department of Botany, University of Allahabad, Prayagraj 211002, U.P., India.

synthesis method of ZnO NPs using leaf extract of *Calendula officinalis* is evidence that it is superior and environmentally friendly method for the preparation of ZnO NPs and hence it can be utilized in various nano-medicine approaches.

Article Highlights

- Green synthesis (hydrothermal method) of ZnO-NPs using leaf extract of *Calendula officinalis L*. and its spectroscopic investigation.
- Found effective Antioxidant activities of green synthesised ZnO that can be employed as skin care and cosmetics.
- Green synthesized ZnO NPs having a significant bactericidal activity observed against bacteria *S. aureus*, *K. pneumonia* and *E. coli*.

Keywords ZnO NPs · FE-SEM · X-RD · Multi-drug resistant · Antioxidant assay · Antimicrobial assay · Etc

1 Introduction

Metal oxide nanoparticles (NPs) have opened a new horizon in the fields of drug delivery, gene delivery, nanomedicine, and biosensing in the twenty-first century [1, 2]. Nanoparticles are also applicable in environmental protection, sensing, communication, cosmetics, medical industry etc. [3]. The magnetic and catalytic properties of nanoparticles, along with their improved surface to volume ratio, can be enhanced by some unique modified processes [4, 5]. Nanoparticles can be synthesized by using an array of physical, chemical, and biological methods. The hydrothermal processes, physical vapor deposition, microemulsion, precipitation, ultrasonic irradiation, chemical reduction, plasma, and sol–gel methods are the best examples of the above methods [6]. But these methods required a variety of hazardous chemicals and a huge amount of energy to synthesize the nanoparticles. The above methods also utilize very high temperatures and pressures, which are very harmful to the environment. Accordingly, the product cast gets very high due to the higher order of the equipment used in these methods [7]. As a result, an environmentally friendly method is required to synthesize the nanoparticles without utilizing any toxic components. Recently, many scholars have taken an interest in preparing the nanoparticles via green route. In medical science, especially in the diagnosis and treatment of several diseases, the biological method via the green route is comparatively more advantageous than the physical and chemical methods. Thus, the biological method via green route has replaced the physical and chemical methods for the synthesis of nanoparticles due to the high energy consumption, low cost, environmental impact, and production of more stable and biocompatible nanoparticles [8, 9]. Moreover, this method controls the morphology of nanoparticles, including nanorods, nanospheres, nanoporous structures, and nanowires, crucial for various emerging potentials applications [10].

Microorganisms [11], enzymes [12], fungi [13], and plant extracts [14] are used to prepare metal and metal oxide nanoparticles. Nevertheless, it is challenging to develop an effective and environment friendly method to prepare nanoparticles with absolute sizes, shapes, and compositions. Nontoxic and environment friendly nanoparticles are prepared by a variable phyto-chemistry based process using biological entities [15, 16]. There are several harmful compounds including radiation, smoke, and pollution; which pose serious effect to human health concern. Antioxidants are being used more frequently in an effort to mitigate the negative effects of these free radicals. Determining the reactive oxygen species (ROS) reaction requires examining the physical and chemical characteristics of nanoparticles, such as their size, surface charge, and chemical makeup. This is important because ROS generation can be control due to the intrinsic properties of nanoparticles. Numerous studies have demonstrated the ability of metal or metal oxide nanoparticles produced with plant extracts to scavenge radicals. These extracts phytochemicals have two functions: they stabilize the nanoparticles and function as antioxidants to combat free radicals [17, 18].

Among the various metal oxide nanoparticles, zinc oxide nanoparticles (ZnO NPs) are one of the most cost-effective metal oxide nanoparticles with minimal toxicity and the highest biocompatibility. Nowadays ZnO NPs are used in photothermal therapy, antibacterial and anticancer drug distributions, cell imaging, and in bio-sensing by making them a promising tool in the field of biomedical sciences [19, 20]. Various methods of synthesis are utilized to improve both the crystal size and their properties for the production of ZnO NPs [21]. Among them, green synthesis method for the preparation of ZnO NPs are widely accepted due to its non-toxicity, environmental friendliness, and wide range of applications viz. antimicrobial properties, antioxidants, anti-aging, anticancer and so on. In the green synthesis method, secondary

metabolites trap the metal ions and act as capping agents that help stabilize the nanoparticles in terms of electrostatic, steric, hydration forces, depletion, and Vander-Waals forces [22, 23]. The interactions of ZnO NPs with microbial cells are possible due to the smaller surface area and higher charge density [24, 25].

Researchers have used a variety of physico-chemical [26, 27] and biological or plant-mediated [28, 29] methods to synthesize the ZnO NPs. Green synthesis becomes more preferable technique in recent decades for producing the metallic nanoparticles because of cost effectiveness, lesser toxicity, and additional environmental suitability [30]. Plant extracts are used by researchers to create ZnO NPs through a green synthesis process. For example, several kind biological extracts including algal seaweeds [31], *Hibiscus sabdariffa* [32] *Limonium pruinosum* [33], *Laurus nobilis* [34], *Rosa indica* [35] *Parthenium hysterophorus* [36], *Thymus spp.* [37], *Solanum nigrum* [38], *Lawsonia inermis* [39], *Syzygium cumini* [40], and *Agathosma betulina* [41]. These natural extracts having stabilizing and reducing agents, play a significant role in the production of ZnO NPs. This chemical free approach of synthesizing nanoparticles is in line with the worldwide movement toward sustainability and is a viable substitute for traditional techniques that mainly rely on hazardous chemicals and energy-intensive procedures.

Calendula officinalis is a flowering plant which belongs to the family of Asteraceae. A wide range of pharmacological effects can be observed in the extract of *Calendula officinalis* due to which it can be utilized as an antiseptic, stimulant, diaphoretic, antispasmodic, and anti-pyretic agent [42, 43]. It has been observed that the leaf extracts of the *Calendula officinalis* have anti-cancerous, antiviral anti-genotoxic, anti-oxidant, anti-microbial and anti-inflammatory properties [44, 45].

The present study is focused on the synthesis of ZnO NPs via the green route by using *Calendula officinalis* leaf extract. The prepared ZnO NPs are further characterized by XRD, FE-SEM, UV–Vis and FT-IR spectroscopy for the size, shape, optical properties and stability of the ZnO NPs, respectively. The study also emphasizes the application approach of these nanoparticles towards medicinal area due to their effectiveness in antimicrobial and antioxidant properties. The antimicrobial study was done against multi-drug resistant human pathogens. Also an antioxidant activity was analyzed against DPPH free radical scavenging properties.

2 Method and reagents

2.1 Chemical products

Zinc acetate dihydrate ($C_4H_6O_4Zn.2H_2O$) (219 g/mol, purity 98.5%), and sodium hydroxide (NaOH) (39.997 g/mol, purity 97%) were supplied by Merck Life Science Pvt. Ltd. Mumbai. Nutrient agar (NA), Mueller Hinton Broth (MHB), Mueller Hinton Agar (MHA) and 2, 2-diphenyl-1-picrylhydrazyl (DPPH) (394.32 g/mol, purity 95%) were procured from Himedia Pvt. Ltd. Mumbai for antibacterial assay. As a solvent deionized water was employed. All the chemicals used in this experiment, are analytical grade.

2.2 Leaves procurement and processing

The fresh *Calendula officinalis* leaves were collected from the Roxburgh Botanical Garden, University of Allahabad, Prayagraj, Uttar Pradesh, India. The *Calendula officinalis* plants were identified by Prof. Anupam Dikshit, Department of Botany, University of Allahabad. Leaves were cleaned three times to get rid of the dust and other contaminants, and left in the shade for a week to dry. Leaves were chopped into small pieces to prepare the leaf extract.

2.3 Preparation of the leaf extract

Chopped *Calendula officinalis* leaves (25 g) were added in 100 ml deionized water and kept on magnetic stirrer for 6 h at 60^0C for 1200 rpm [46]. The aqueous solution was filtered using filter paper and kept for 24 h at 4^0C. The zinc ions which are supportive to form the ZnO NPs, were reduced from the fused aqueous extract and zinc acetate.

2.4 Green synthesis of ZnO NPs

A beaker of *Calendula officinalis* leaf extract (50 ml) was kept on magnetic stirrer (1200 rpm) at 60^0C temperature. The aqueous solution of $ZnC_4H_6O_4.2H_2O$ (0.45 M of 50 ml) was dropped continuously and stirring it for two hours with constant stirring (1200 rpm). The colour of the reaction mixture started converting in to brown precipitate. The resulting precipitate was centrifuged at 6000 rpm for 15 min. It was washed twice with deionized water before spending the entire night at 100^0C [47]. Figure 1 shows the systematic procedure of synthesis of ZnO NPs.

2.4.1 Mechanism for the green synthesis of ZnO NPs

Phytochemicals in plant extracts can reduce metal precursors to nanoparticles, acting as both reducing and stabilizing agents. *Calendula officinalis* leaf extract contains numerous phytochemicals including triterpenes, Flavonoids, Phenolic compounds, coumarins, and carotenoids, which play a significant role in the reduction of metal ions. The concentration of these phytochemical reducing agents varies in different plant extracts, significantly influencing the composition of leaf extract in the process of the formation of nanoparticles. Apart from it various factor such as pH, temperature, contact time, metal salt concentration, and the phytochemical profile of the plant extract impact the synthesis, stabilization, and quantity of nanoparticles produced. Jaychandran et al. [48] suggested that metal ions undergo encapsulation with an organic covering in three steps for stabilization after reduction by plant extracts: 1) Activation phase, involving metal

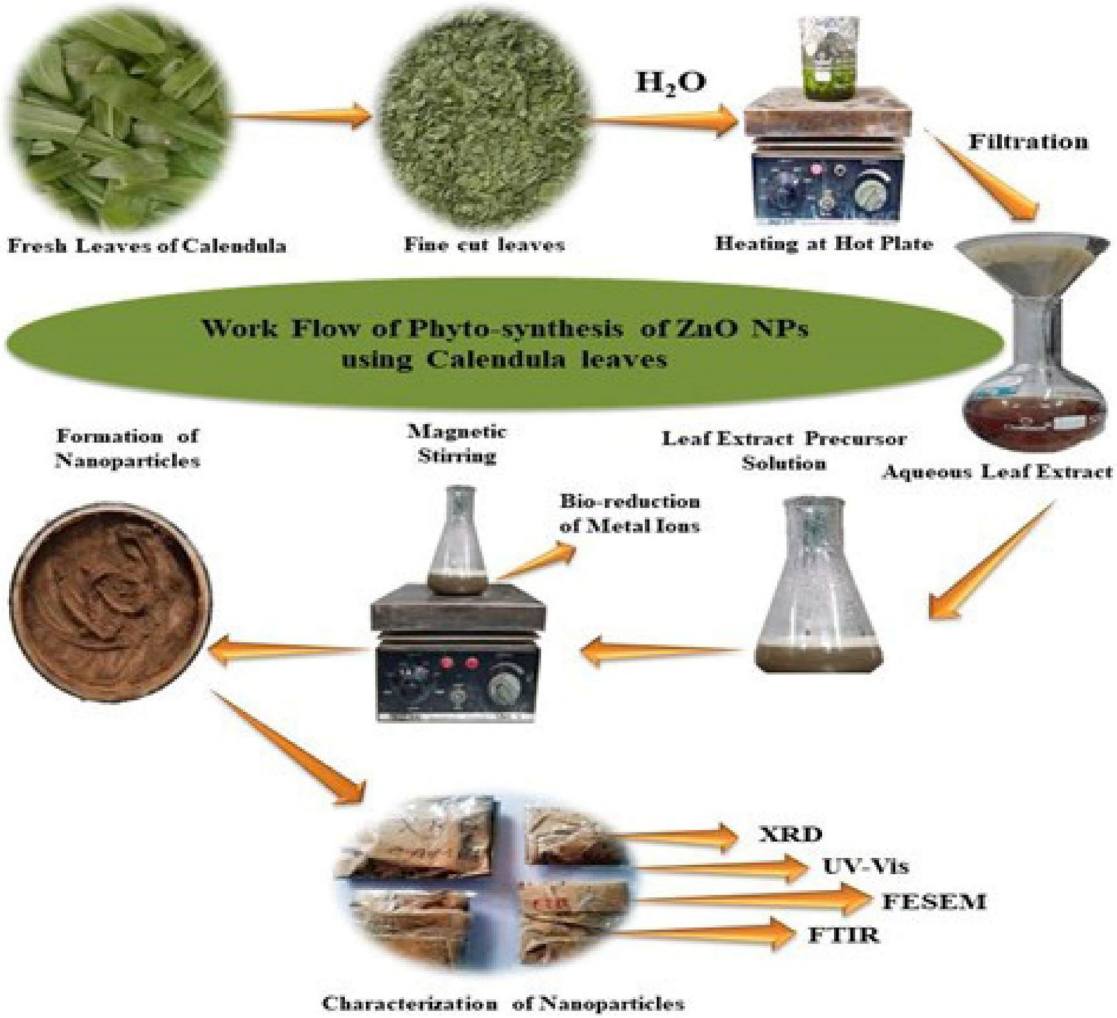


Fig. 1 Flow diagram of synthesis of ZnO NPs using leaf extract of *Calendula officinalis*

ion reduction and nucleation, 2) Growth phase, ensuring nanoparticle stability, 3) Termination phase, determining the shape of nanoparticles. Metals like copper, silver, gold, titanium, zinc, iron, and nickel form metal oxides through phytochemical activity. Phytochemicals enable metal ions to reach growth and stabilization, ultimately linking metal ions and defining their shape [48]. The clear cut mechanism of green synthesis of ZnO NPs using *calendula officinalis* leaf extract, is represented in Fig. 2.

2.5 Spectroscopic investigation of ZnO NPs

2.5.1 X-Ray powdered diffraction (XRD) analysis

The X-Ray powder diffraction technique was used to investigate the crystalline structure, size and formation of the compounds. ZnO NPs which were synthesized via the green route using *Calendula officinalis* leaf extract were analyzed using single crystal X-Ray Diffractometer (Rikagu, Ultima IV Japan) with Cu-Kα radiation (λ = 1.54020 Å). The scanning was done in the region of 2*θ* from 20° to 70°.

2.5.2 Field emission-scanning electron microscopy (FE-SEM)

The surface morphology of synthesized ZnO NPs were further analyzed by FE-SEM (JEOL India Pvt. Ltd., Delhi India) for superficial phenotype. A very small amount of nano-powder was kept on the carbon coated copper grid, and then FE-SEM grid was dried with a fine layer of sample and fixed with gold for 5 min.

2.5.3 Fourier transform infra-red (FT-IR) spectroscopy

The Perkin-Elmer Bucking Hamashire, UK FT-IR spectroscopy was used to investigate bond and functional groups existing in the green synthesized ZnO NPs. During the analysis, the band and fictional group were identified by using FT-IR spectra with a resolution of 4.0 cm^{-1} in order to 4000–450 cm^{-1}.

2.5.4 Ultraviolet–Visible (UV–Vis) spectroscopy

The optical properties of the green synthesized ZnO NPs were investigated using UV–Vis spectroscopy. The shape and size of the synthesized ZnO NPs, affect the sharpness of the absorption peak. In order to check the optical properties of green synthesized ZnO NPs, 0.05 g of ZnO NPs was dispersed in 4 mL of double ionized water. The absorption spectrum was recorded using an UV–Vis spectrophotometer (Spectra Max, San Jose, CA, USA) in a wavelength range of 350–460 nm.

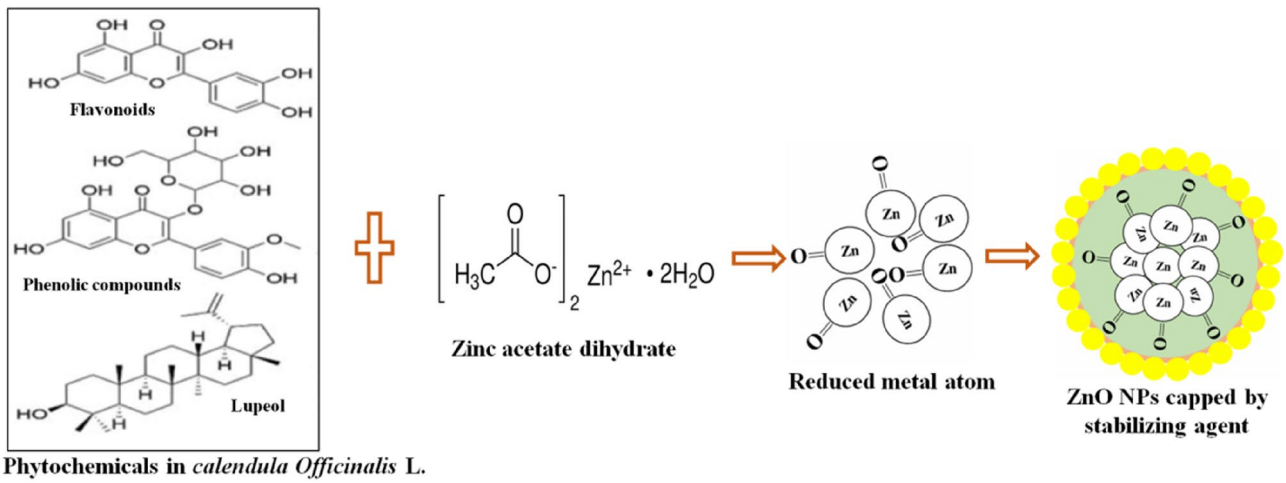


Fig. 2 Mechanism for the synthesis of ZnO NPs using *Calendula officinalis* leaf extract

2.6 Free radical scavenging activity

Brand William conducted a comprehensive investigation into the free radical scavenging activity of ZnO nanoparticles (NPs) synthesized through green methods, with adaptations made to the protocol outlined by a prior study [49]. The 2, 2-diphenyl-1-picrylhydrazyl (DPPH) radical, known for its stable purple color and characteristic absorption peak at 517 nm, served as the substrate for this assessment. Upon exposure to antioxidants present in the medium, the purple hue of DPPH underwent a discernible transition to transparency, indicative of radical scavenging activity. To prepare the solution for the antioxidant assay, 39.44 mg of DPPH was dissolved in 100 ml of methanol, yielding a concentration of 0.14 mM. Similarly, stock solutions of green-synthesized ZnO NPs and standard ascorbic acid were prepared in methanol, followed by appropriate dilutions to achieve the desired working concentrations. Ascorbic acid, employed as the standard, underwent evaluation at concentrations spanning 2–6 µg/ml to establish a calibration curve. In a controlled environment within a darkened laboratory, 140 µl of freshly prepared 1 mM DPPH was combined with 860 µl of test samples. To minimize the influence of ambient light, all test tubes were carefully wrapped in aluminum foil. A comparative analysis was conducted using a control sample comprising 1 ml of DPPH solution mixed with 3 ml of methanol. Data interpretation involved calculating the percent inhibition of DPPH free radicals relative to the control, with further determination of IC50 values derived from the descending order of test sample readings. This meticulous approach enabled a thorough assessment of the antioxidant potential of the green-synthesized ZnO NPs and facilitated valuable insights into their free radical scavenging capabilities. The percentage of scavenging free radical values was calculated by the following formula-[50]

$$\%\textbf{Radicals cavenging activity} = \frac{\text{Absorbance of blank} - \text{absorbance of sample}}{\text{Absorbance of blank}} \times 100$$

2.6.1 Antioxidant radical power

The antioxidant radical power of the green synthesized ZnO NPs and Ascorbic acid can be evaluated by the given formula [51]

$$\text{ARP} = \frac{1}{\text{EC}_{50}} \tag{1}$$

2.7 Antibacterial activities

The antibacterial assessment employed the widely recognized disc diffusion method to discern the efficacy of green-synthesized ZnO nanoparticles (NPs) against three distinct bacterial strains: *Staphylococcus aureus* (Gram positive), *Escherichia coli* (Gram negative), and *Klebsiella pneumoniae* (Gram negative). These bacterial strains represent diverse microbial morphologies and pathogenic profiles, allowing for a comprehensive evaluation of the nanoparticles' antibacterial potential across different bacterial types. Prior to testing, the green-synthesized ZnO NPs were meticulously dissolved in dimethyl sulfoxide (DMSO) to facilitate the creation of standardized stock solutions, ensuring consistency and accuracy in subsequent analysis. This step is crucial in maintaining the stability and reproducibility of the experimental conditions, thereby enhancing the reliability of the results obtained. In a controlled laboratory environment, cultures of the respective bacterial strains were inoculated into separate batches of nutrient broth and then subjected to an incubation period of 12 h at 37°C. This incubation duration allows for optimal bacterial growth, ensuring that the cultures reach a logarithmic phase of growth before further experimentation. Following incubation, 100 µL of each bacterial culture was uniformly spread onto sterile Muller-Hinton agar (MHA) plates using sterile swabs. The choice of MHA as the growth medium is deliberate, as it provides a standardized and optimal environment for bacterial growth, enabling accurate assessment of antibacterial activity. Subsequently, discs impregnated with varying concentrations (50, 75, and 100 µg/ml) of green-synthesized ZnO NPs were carefully placed onto the agar plates, with sterile water discs serving as negative controls. This setup allows for the assessment of dose-dependent antibacterial effects, elucidating the relationship between NP concentration and inhibitory activity. The plates were then incubated at 37°C for a period of 24 h to allow for bacterial growth and subsequent assessment of inhibition zones [47]. The formation of clear zones of inhibition around the NP-loaded discs indicates the antibacterial activity of the synthesized nanoparticles against

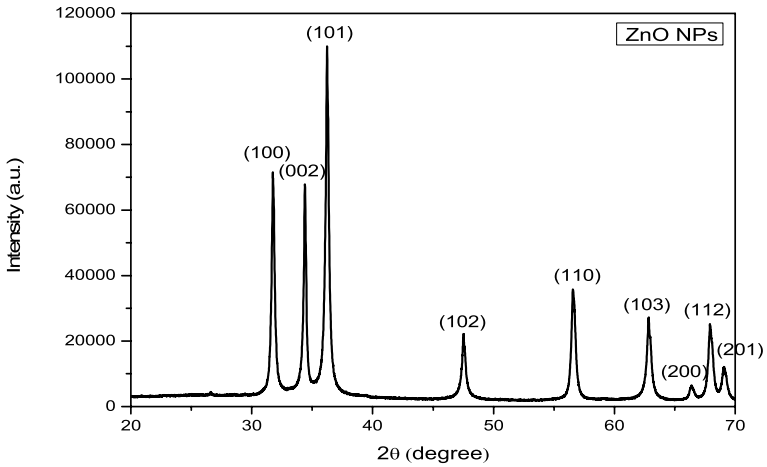


Fig. 3 XRD pattern of green synthesized ZnONPs

Table 1 XRD analysis at various diffraction angles

S. No	2θ	FWHM (β) (degree)	Miller indices	Particle size (D), (nm)
1	31.6°	0.2935	(100)	29.36
2	34.3°	0.2976	(002)	29.16
3	36.1°	0.3089	(101)	28.23
4	47.4°	0.3754	(102)	24.12
5	56.4°	0.4039	(110)	23.29
6	62.7°	0.4308	(103)	22.54
7	66.2°	0.4606	(200)	21.49
8	67.8°	0.4669	(112)	21.40
9	69°	0.4834	(201)	20.81

the respective bacterial strains. To ensure the reliability and robustness of the experimental data, each assay was performed in triplicate, minimizing experimental variability and enhancing the statistical significance of the findings [47]. The inhibition zone diameters were meticulously measured, and the data were expressed as mean values ± standard deviation, providing a comprehensive understanding of the antibacterial efficacy of the green-synthesized ZnO NPs.

3 Results and discussion

3.1 X-ray diffraction analysis of green synthesized ZnO NPs

The recorded X-ray diffraction pattern shows the phase and crystallinity of the produced ZnO NPs. The produced ZnO NPs XRD patterns are displayed in Fig. 3. Lattice planes (hkl) of (100), (002), (101), (110), (200), (112), and (201) could be responsible for the diffraction peaks at 31.6^0, 34.3^0, 36.1^0, 47.4^0, 56.4^0, 62.7^0, 66.2^0, 67.8^0, and 69^0 (Table 1) for the hexagonal wurtzite ZnO phase (JCPDS-file: 36–1451) [52]. Furthermore, the complete conversion of the Zn precursor into ZnO NPs is shown by the lack of an impurity peak in the diffraction pattern. *Calendula officinalis* leaf extracts phenols and flavonoids work as reducing agents and shield the zinc acetate molecule's outermost surface, they promote the development of ZnO NPs. Diffraction peaks that are both conspicuous and narrow indicate that the product's particles have a distinct crystalline structure. The strong peak intensity indicates the high crystalline nature of the produced ZnO NPs. The Debye-Scherer equation is used to further estimate the diameter of the produced ZnO NPs [53].

$$D = \frac{K\lambda}{\beta Cos\theta} \tag{2}$$

where: D = Average crystallite size of the particles, K = Debye-Scherer's constant (= 0.94), λ = Wavelength of the Cu Kα-radiation (= 0.1540 nm), β = Full width at half maximum (FWHM) in radian, θ = Bragg's diffraction angle.

The XRD analysis proves that the *Calendula officinalis* leaves are the effective reducing agents for the green synthesis of ZnO NPs.

The FWHM of the most intense peak, which corresponded to the (101) plane located at 36.1°, was used to compute the crystallite diameter of the generated ZnO NPs, which came out to be 28.23 nm. ZnO NPs were found to have a well-crystalline character and a hexagonal wurtzite crystal structure. After calculations, it was discovered that the lattice has dimensions of (a = b) = 3.2535 Å and (c = 5.2151 Å).

The change in crystallographic properties can also be understood with the help of W–H plot between βCosθ versus 4Sinθ. Figure 4 depict W–H plots from mathematical relations-

$\beta Cos\theta = \frac{k\lambda}{D} + 4\mu_s Sin\theta$ (2).

Strain is determined from the slope of straight line. The values of micro-strain have been calculated and found to be 0.00451. The reciprocal of intercept reveals the grain size of the sample. The variations of grain sizes calculated from both Debye-Scherer's as well as W–H plot are approximately the same.

3.2 FE-SEM analysis of green synthesized ZnO NPs

The generated ZnO NPs FE-SEM images are displayed in Fig. 5. The surface morphology displays the aggregated particulates. FE-SEM provides the microstructure and surface morphology of samples and XRD provides the sample's crystallite size. From FE-SEM image of ZnO NPs, it is revealed that most of the particles are spherical in shape. Surface morphology also provides evidence that ZnO NPs were formed in their agglomerated state [54]. The microstructures have varying sizes, as seen by the FE-SEM image (Fig. 5).

The histogram of the FE-SEM image is formed by IMAGE-J software. The histogram gives statistics about the distribution of pixel values in the whole image. Histogram of FE-SEM images is made by IMAGE-J. The software program Image J (version 1.46r) was used for FE-SEM image analysis. The observed standard deviations and mean deviations of ZnO NPs using Image-J software were found to decrease with increasing the magnification from × 200 to × 1100 (Fig. 6). The standard deviation (51.287) revealed that pixels spread out around the mean of the crystallite of ZnO NPs. The mean deviation (127.148) was measured as the closest alternative to the standard deviation.

Thus, the instability of the FE-SEM micrograph was expressed as the significance of the standard deviation. The observed irregular-shaped nanoparticles in FE-SEM images indicated that green synthesized nanoparticles using leaf extract contained a large volume-to-surface ratio. The histogram of the FE-SEM image showed that the ZnO NPs at different magnifications had a uniform particle size distribution on the surface of the cluster.

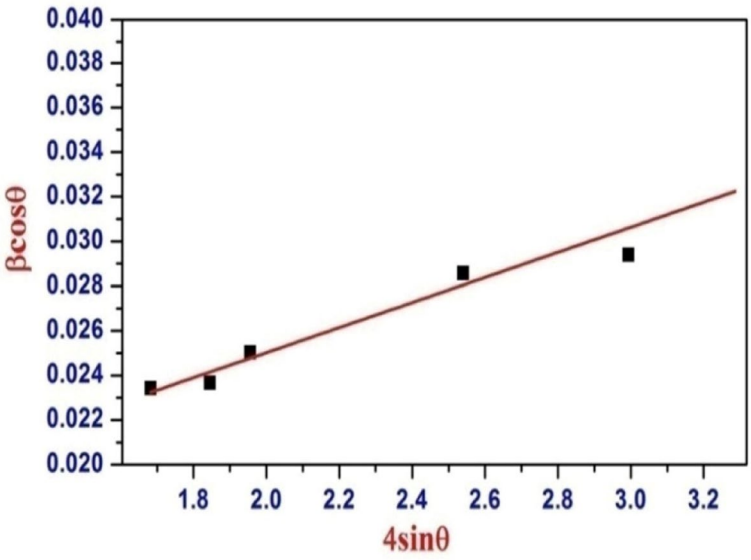


Fig. 4 Williamson-Hall (W–H) Plot for green synthesized ZnO NPs

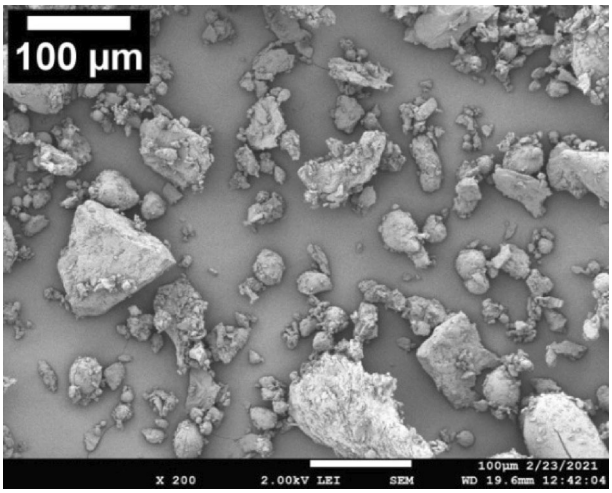


Fig. 5 FE-SEM micrographs of green synthesized ZnO NPs

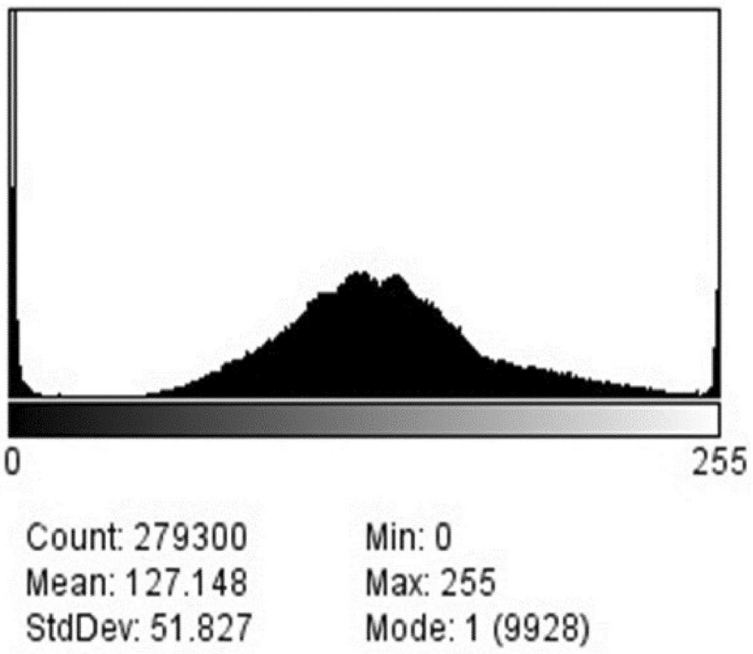


Fig. 6 Histogram of SEM images by IMAGE-J gives the information of microstructure particle distribution in the pixel values

3.3 FT-IR analysis of green synthesized ZnO NPs

Figure 7 shows the FT-IR spectrum of the green synthesized ZnO NPs. From the spectrum it is clear that the compositional and functional groups are present in the green synthesized ZnO NPs. The spectroscopic grade KBr was utilized in the form of a pallet to record the FT-IR spectrum in the wave number range of 4000–500 cm^{-1} in the different reflectance modes. FT-IR spectrum has shown the numerous bands at various absorption peaks (Table 2, Fig. 7) which are similar to the ones earlier reported [55, 56]. To be more precise, an extensive band at 3401 cm^{-1} is assigned to the O–H stretching mode of the hydroxyl group present in the green synthesized ZnO NPs. The peak of 3080 cm^{-1} is due to the C-H stretching vibration of alkenes functional groups. The peaks detected in spectrum (Fig. 7) at 2345 cm^{-1} assign the C = C alkane/C = N stretching.

However, the peak at the 1569 cm^{-1} is assigned to the (N–H) stretching of the amine functional group and 1423 cm^{-1} is assigned to the (C-O), C-F, alkyl halide strong groups present in the green synthesized ZnO NPs. Probably 1022 cm^{-1}, 948 cm^{-1}, 773 cm^{-1}, 688 cm^{-1} is assigned the C-N stretching amine functional group which are present synthesized ZnO NPs [57]. The FT-IR spectrum confirms the formation of chemical bonding due to functional groups present in the green synthesized ZnO NPs.

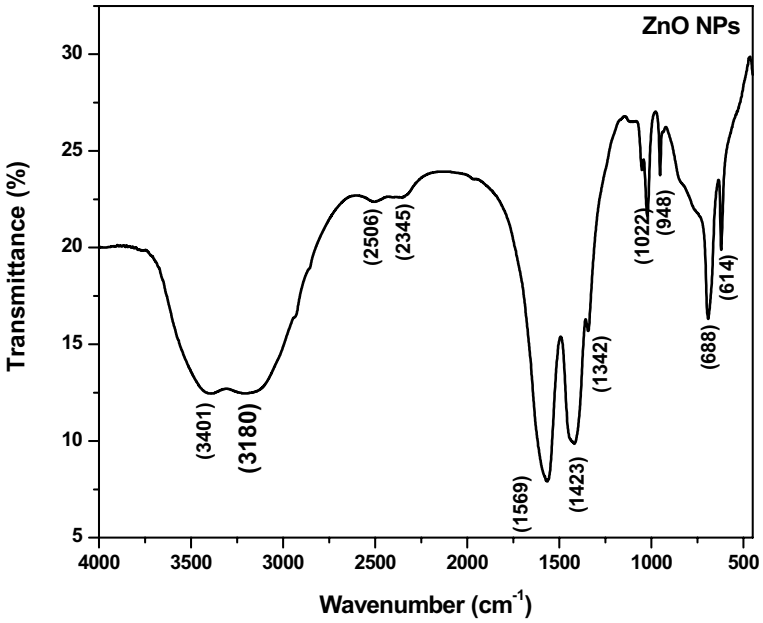


Fig. 7 FT-IR spectra of green synthesized ZnO NPs

Table 2 Bond and functional group present in FTIR spectra

S.N	Absorption peak (cm^{-1}) of ZnO NPs	Bond and functional groups
1	3401	O–H stretch of alcohol phenol
2	3180	C–H stretching of alken
3	2345	C=C/alken-C=N stretching
4	1569	C–H stretching of amine
5	1423	(C–O), C-F, alkyl halide strong
6	1022	C–N Stretching amine or Phenols
7	948	C – N stretching C–N Stretching amine
8	773	C–N Stretching amine
9	688	C–N Stretching amine
10	614	C–N Stretching amine

3.4 UV–Visible analysis of green synthesized ZnO NPs

The leaves extract not only acts as a reducing agent but also a stabilizing agent. The zinc ions are reduced in the zinc oxide solution by the secondary metabolite of the plants. This was studied by taking the UV-Vis spectrum in between 350 nm and 460 nm. Figure 8 showed the absorption spectrum of green synthesized ZnO NPs. Two strong absorption peaks were visualized at 355 nm and 370 nm which confirmed the formation of ZnO at nanoscale [58]. For the formation of ZnO NPs, the absorbance peak was found in the previous report in the range of 300–360 nm [59]. The smaller size particles were also visualized at FE-SEM image (Fig. 5) that also supported the above statement and bump around 370 nm. This was because of more interaction of Zn ions with secondary metabolites. Bioactive constituents of plant extract interacted with the Zn ions and acted as stabilizing as well as abbreviating agents in the reduction of the metal size [60, 61]. The band gap energy was evaluated by equation-

$$E_g = \frac{1240}{\lambda} eV \tag{3}$$

The optical band gap energy of green synthesized ZnO NPs were observed 2.986 eV (Fig. 9) which was comparable to the previously reported one [62, 63]. As ZnO is a direct wide band-gap (2.986 eV) semiconductor material at a room temperature, it has gained widespread research interest for a variety of applications such as, optical and

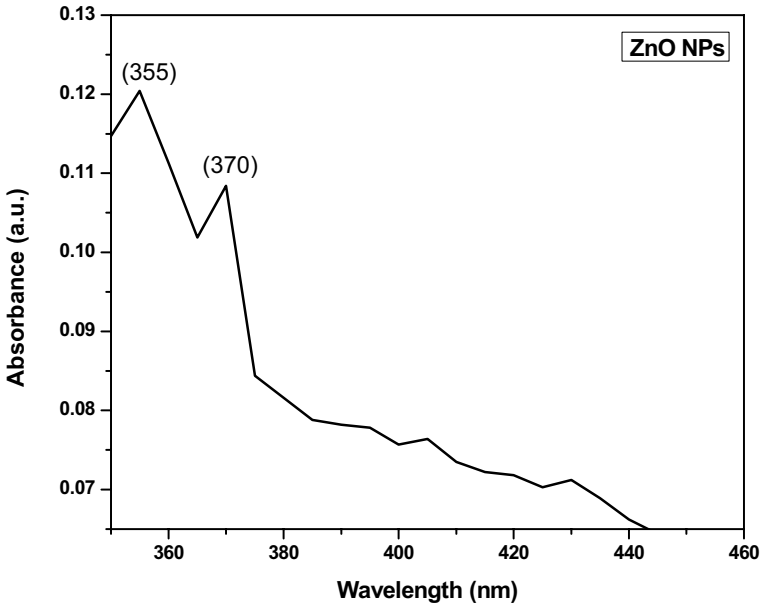


Fig. 8 UV–Visible Spectrum of green synthesized ZnO NPs

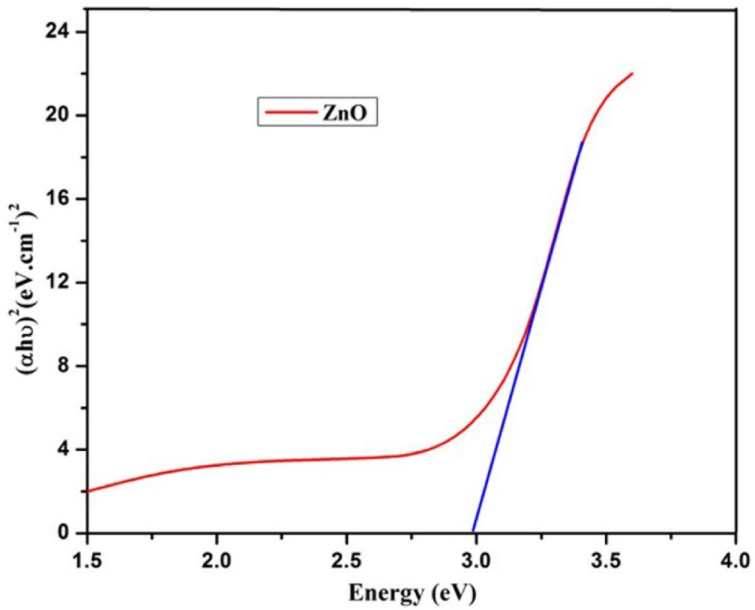


Fig. 9 Optical band gap of green synthesized ZnO NPs

opto-electronic devices because of its intriguing features including non-toxicity, non-expensive, large electron mobility and various novel morphological features.

3.5 Free radical scavenging activity:

The evaluation of antioxidant activity entailed assessing the DPPH-mediated free radical scavenging capability of ZnO NPs. DPPH, a stable nitrogen-centered free radical, readily undergoes electron or proton transfer, converting into a stable diamagnetic free radical. Consequently, the purple color of the DPPH solution diminishes in proportion to the electrons received from antioxidant agents like ZnO NPs, resulting in the formation of 1, 1-diphenyl-2-picryl-hydrazine with a light yellowish colour. The remarkable antioxidant prowess of green-synthesized ZnO NPs arises from their ability to transfer electrons from oxygen to the electron density of nitrogen within DPPH, effectively neutralizing its unpaired electron. This electron transfer process engenders an electronegative force, which is particularly pronounced in ZnO NPs and hinges upon the structural configuration and oxygen moiety.A

Table 3 Antioxidant reducing power (ARP)

S. No	Samples (drug)	ARP	R^2 value
1	*Ascorbic acid*	*0.22142*	*0.9866*
2	*ZnO NPs*	*0.33157*	*0.9156*

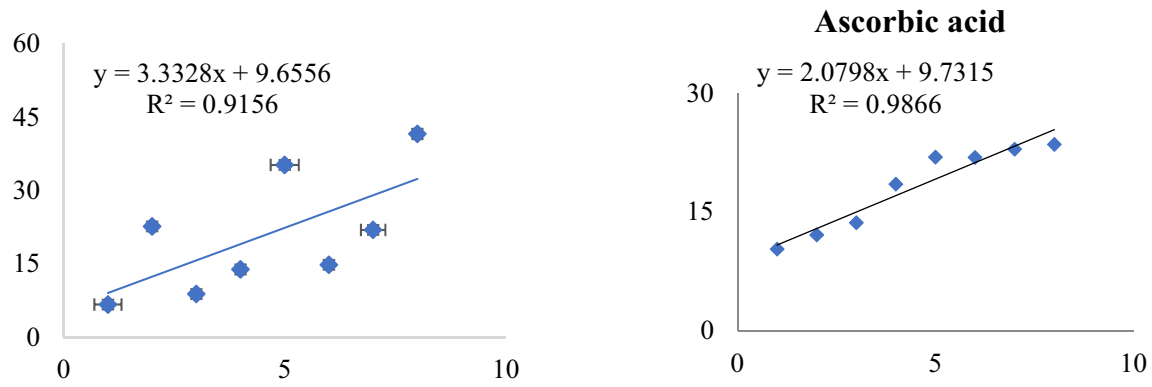


Fig. 10 Free radical scavenging activity of ZnO NPs and Ascorbic acid against DPPH

pivotal aspect of green-synthesized NPs lies in the electrostatic interaction between negatively charged bioactive compounds sourced from plant extracts and positively charged metal ions within the NPs. This interaction enhances the antioxidant activity manifold compared to chemically synthesized counterparts. In this context, the IC_{50} value, derived from the mediated antioxidant assay, stands at 6600 µl/ml. Discrepancies in the antioxidant activity of ZnO NPs originating from different sources can be attributed to variations in size and surface characteristics due to the synthesis process and the botanical origins. Previous studies have underscored that smaller-sized ZnO NPs exhibit the highest percentage of radical scavenging activity, a trend paralleled in gold nanoparticles as well. This emphasizes the nuanced interplay between nanoparticles properties and antioxidant efficacy, thereby highlighting the significance of synthesis methodologies and precursor materials in dictating the antioxidant potential of nanomaterials. Over all, the utilization of nano-sized ZnO particles represents a strategic approach to bolstering antioxidant activity through synergistic interactions, enhanced reactivity, and size-dependent effects. In recent study green synthesized dual doped Co–Cu from plant *Tinospora cordifolia* exhibited a remarkable antioxidant activity against DPPH, HO and NO free radicals [64]. In another study Cu-doped hematite nanoparticles was created through green synthesis from the plant *Azadirachta indica* leaves extract used to examine the antioxidant activities and doped hematite nanoparticles contains high amount of free radical scavenging activity against DPPH free radicals [65]. In some advanced study iron oxide nanoparticles (Fe_2O_3-NPs) were synthesized by chemical and green precipitation methods had been tested against photo-catalytic and antioxidant activities was significantly high of green synthesized nanoparticles of *Azadirachta indica* [66].The green synthesized nanoparticles from *A. indica* used to create hematite nanoparticles with varied Co/Cu dopant concentrations. Methyl orange and Methylene blue industrial wastes can be degraded by using Co/Cu doped hematite nanoparticles. It also possessed remarkable photo-catalytic and antioxidant activities [67]. Incorporating these nanoparticles into antioxidant formulations holds immense potential for developing novel therapeutics and functional materials aimed at combating oxidative stress-related diseases and promoting overall health and well-being [68].

3.6 Antioxidant reducing power

The antioxidant values also evaluated in terms of ARP values showed 50% scavenging concentration of both the ascorbic acid and ZnO NPs (Table 3 Fig. 10). Approximately the values of 50% scavenging of free radical are equal to ascorbic acid which showed that the ZnO NPs are also potent scavengers of antioxidants [69]

3.7 Antibacterial activity

The antibacterial activities were performed using the disc diffusion method. The disc diffusion method has several limitations such as: 1. It provides primary confirmation of the antibacterial activity but fails to provide accurate cytotoxicity. 2. It is not able to provide the exact minimum inhibitory concentration (MIC) of targeted nanoparticles. 3. It is also not able to depict mechanistic cytotoxicity against the pathogens. Thus our study is only focused to confirm the antibacterial property of ZnO NPs. Apart from these limitations this method have positive approach such as simple, effective and convenient method to check the antibacterial property of a test sample. It also provide effective concentration or lethal concentration (not accurately) of a test sample [70]. The different concentrations of green synthesized ZnO NPs were tested against the pathogenic bacteria, i.e., *S. aureus* (Gram + ve) *E. coli* (Gram -ve), and *K. pneumoniae* (Gram -ve). The green synthesized ZnO NPs were observed against these bacteria, as indicated in Table 4 and Fig. 10. For the standard drug, amoxicillin was taken for reference and for the comparison of the activity of ZnO NPs. Double-distilled water was used as a negative control. ZnO NPs showed maximum inhibition against *Staphylococcus aureus* (35.2 mm ± 0.9) and minimum inhibition against *Klebsiella pneumoniae* (23.6 mm ± 0.1) and *E. coli* (13.5 mm ± 0.1). The efficacy of inhibition percentage is directly proportional to concentration, which means increasing concentration will increase the zone of the diameter [71]. The results reveal that the diameter of the inhibitory zone increases with increasing nanoparticles concentration for all tested strains [71]. It is also observed that the green synthesized ZnO NPs showed better inhibition against Gram + ve in comparison to gram-ve. This may be, the size of nanoparticles was less than 22 nm. which increase its cell membrane penetration property and cause severe cell toxicity (antibacterial property). It is reported that, in metal oxide nanoparticles such as ZnO NPs, the size of nanoparticles is inversely proportional to effective antibacterial property which means lesser the size of nanoparticles couses more antibacterial property [72] This might be because the cell wall of gram-negative bacteria is more complex than that of gram-positive bacteria [2]. Here, the presence of ZnO NPs leads to damage the cell wall of *S. aureus* (Fig. 11). This effect can be explained by the strong direct interactions with the bacterial membrane surface and antibacterial agents like ZnO NPs. For the ZnO NPs to penetrate the bacteria's cells, the bacteria's membrane has small pores [71]. ZnO NPs cause cell harm by encouraging microorganisms to emit reactive oxygen species once they have broken through a membrane [71]. The antibacterial efficacy can be explained based on literature by free radical formations like singlet oxygen, H_2O_2, hydroxyl radicals, and Zn^{2+} ions which are released from the surface of ZnO NPs and damage the cell wall, they damage DNA, and create pores in the membrane where bacteria's can't survive [72]. UV and visible rays can activate ZnO and form electron–hole pairs (e-/h +). It has also been reported that the presence of both these findings demonstrate that ZnO NPs are hazardous to the tested bacterial strains [73, 74]. This means that they have great potential as an antibacterial agent in commercial and medical settings.

Green synthesized ZnO NPs using *Calendula officinalis* is found more effective than the previous studies. Hence green synthesized ZnO NPs can be utilized effectively in various biomedical applications including skin care, ointment, and cosmetics. The present study is focused on antioxidant and antibacterial analysis of the green synthesized ZnO NPs. The antibacterial assay done against *S. aureus, K. pneumonia,* and *E. coli* pathogenic bacteria which is supported by different researcher (Table 5).

Table 4 Depicting the values of antibacterial analysis

Pathogens	ZnO NPs Conc. (µg/ml)	MIC (µg/ml)	Standard (µg/ml)
Staphylococcus aureus	50 µg/ml	22.8 ± 0.3	21.4 ± 0.5
	75 µg/ml	23.6 ± 0.7	
	100 µg/ml	35.2 ± 0.9	
Klebsiella pneumoniae	50 µg/ml	12.4 ± 0.3	22.8 ± 0.8
	75 µg/ml	16.8 ± 0.6	
	100 µg/ml	23.6 ± 0.1	
E.coli	50 µg/ml	10.6 ± 0.6	18.6 ± 0.3
	75 µg/ml	12.7 ± 0.8	
	100 µg/ml	13.5 ± 0.1	

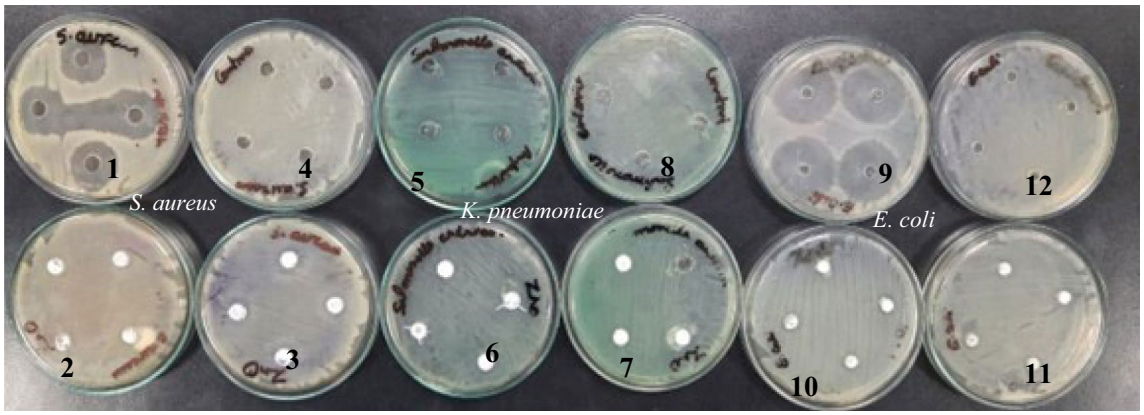


Fig. 11 Bacterial cultures showing the inhibition zones of green synthesized ZnO NPs. against bacteria *S. aureus* (1–3), *K. pneumonia* (5–7) and *E. coli* (9–11) with control (4, 8, 12)

Table 5 Comparative zone of inhibition from previously reported work

Materials	Pathogens	Concentration of ZnO NPs (µg/ml)	Zone of inhibition (mm)	Refrence
ZnO using *M. paniculata L*	*S. aureus*	1000	24	[47]
ZnO using *P. alba*	*S. aureus*	100	20.4	[71]
ZnO using *Strychnos nuxvomica L*	*S. aureus*	400	16	[74]
ZnO using *Canthium dicoccum (L.)*	*S. aureus*	1000	15	[75]
ZnO using *Calendula officinalis L*	*S. aureus* *K. pneumnia E. coli*	50 75 100	35.2 23.6 13.5	Present study

Conclusion

Several methods have been introduced to synthesize ZnO NPs, but recently, biological methods have been advanced over physico-chemical approaches due to their lower energy consumption, cost-effectiveness, and eco-friendliness. The present work enlightened the ZnO NPs using an aqueous greenery extract of *Calendula officinalis*. The secondary metabolites of plant extracts provide stabilizing agents for the synthesis. The optical prosperities, stability, structural characteristics, and morphology of the green synthesized ZnO NPs were analyzed. The FE-SEM micrograph showed that most of the synthesized ZnO NPs have a spherical in shape. The crystalline sizes of the synthesized ZnO NPs were evaluated using Debye-Scherer formula along the most intense peaks (101) and found to be 28.23 nm. FT-IR studies clearly showed the oxide of zinc and bioactive photochemical present in the synthesized nanomaterials which indicate the possibility of formation of ZnO NPs pore shell. The optical band gap energy was evaluated 2.986 eV which can be employed in various optical applications. Furthermore, ZnO NPs were analyzed as an antioxidant against DPPH and antibacterial properties against several multidrug resistance pathogens. The antioxidant reducing power (ARP) value of green-synthesized ZnO NPs was found to be less than that of ascorbic acid. However, despite having a lower ARP value, the experimental results indicate that green-synthesized ZnO NPs exhibit more antioxidant properties than the standard drugs. The antimicrobial activity of green-synthesized ZnO NPs against both Gram-positive (*S. aureus*) and Gram-negative bacteria (*K. pneumoniae* and *E. coli*) was positive. The above studies suggested that synthesized ZnO NPs can be employed in various fields including pharmaceuticals, cosmeceuticals, environmental industries, and biomedical applications. This study would be a promising avenue for further research and development.

Acknowledgements Authors are feeling gratitude to Prof. Ravindra Dhar, Department of Material Science, University of Allahabad for XRD; Dr. Subodh Kumar, Birbal Sahni Institute of Palaeosciences, University of Lucknow, Lucknow for FE-SEM; Dr. Vivek Bhadoria, Ewing Christian College, University of Allahabad for FT-IR. Also feeling grateful to the Head, Department of Botany, University of Allahabad for providing lab facility.

Author contributions The study's conception and design were contributed by all authors. Material preparation, data collection and writing were conducted by Ajay Kumar Tiwari, Saket Jha, and Rohit Shukla. The spectroscopic investigations were performed by Ajay Kaumr Tiwari, and Ram Raseele Awasthi. The antioxidant and antimicrobial activities were performed by Sharad Kumar Tripathi, Abhishek Kumar Bhardwaj, and Saket

Jha. The initial draft of the manuscript was composed by Ajay Kumar Tiwari and Saket Jha. Review, Editing, and Supervision of the manuscript was composed by Abhimanyu Kumar Singh, and Anupam Dikshit. Authors have contributed feedback and approved for the final manuscript.

Data availability The experimental data and the results that support the findings of this study are available.

Declarations

Ethics approval and consent to participate Not applicable.

Consent for publications Not applicable.

Competing interests The authors declare that they have no known competing financial interests or personal relationships that could have appeared to influence the work reported in this paper. There is no conflict of interest in this manuscript. The authors declare that they have no known competing financial.

Open Access This article is licensed under a Creative Commons Attribution 4.0 International License, which permits use, sharing, adaptation, distribution and reproduction in any medium or format, as long as you give appropriate credit to the original author(s) and the source, provide a link to the Creative Commons licence, and indicate if changes were made. The images or other third party material in this article are included in the article's Creative Commons licence, unless indicated otherwise in a credit line to the material. If material is not included in the article's Creative Commons licence and your intended use is not permitted by statutory regulation or exceeds the permitted use, you will need to obtain permission directly from the copyright holder. To view a copy of this licence, visit http://creativecommons.org/licenses/by/4.0/.

References

1. Ananthalakshmi R, Rajarathinam SR, Sadiq AM. Antioxidant activity of ZnO Nanoparticles synthesized using Luffa acutangula peel extract. Res J Pharm Technol. 2019;12(4):1569–72. https://doi.org/10.5958/0974-360X.2019.00260.9.
2. Bhardwaj AK, Sundaram S, Yadav KK, Srivastav AL. An overview of silver nano-particles as promising materials for water disinfection. Environ Technol Innov. 2021;23: 101721. https://doi.org/10.1016/j.eti.2021.101721.
3. Ijaz I, Gilani E, Nazir A, Bukhari A. Detail review on chemical, physical and green synthesis, classification, characterizations and applications of nanoparticles. Green Chem Lett Rev. 2020;13(3):223–45. https://doi.org/10.1080/17518253.2020.1802517.
4. Tiwari AK, Jha S, Singh AK, Mishra SK, Pathak AK, Ojha RP, Dikshit A. Innovative investigation of zinc oxide nanoparticles used in dentistry. Crystals. 2022;12(8):1063. https://doi.org/10.3390/cryst12081063.
5. Ramos AP, Cruz MA, Tovani CB, Ciancaglini P. Biomedical applications of nanotechnology. Biophys Rev. 2017;9(2):79–89. https://doi.org/10.1007/s12551-016-0246-2.
6. Singh MP, Bhardwaj AK, Bharati K, Singh RP, Chaurasia SK, Kumar S, Vikram K. Biogenic and non-biogenic waste utilization in the synthesis of 2D materials (graphene, h-BN, g-C2N) and their applications. Front Nanotechnol. 2021;3:685427. https://doi.org/10.3389/fnano.2021.685427.
7. Bhardwaj AK, Naraian R. Cyanobacteria as biochemical energy source for the synthesis of inorganic nanoparticles, mechanism and potential applications: a review. Biotech. 2021;11(10):445. https://doi.org/10.1007/s13205-021-02992-5.
8. Mittal R, Sharma A, Bhardwaj AK, Bhateria R, Bansal S, Kashyap R, Bhukal S. Removal of chromium (VI) using spirulina assisted synthesized mesoporous iron oxide nanoparticles. Inorg Chem Commun. 2023. https://doi.org/10.1016/j.inoche.2023.110881.
9. Debroy A, Joshi S, Yadav M, George N. Green synthesis of nanoparticles from bio-waste for potential applications: Current trends, challenges, and prospects. Bio-Based Mater Waste Energ Generation Res Manage. 2023. https://doi.org/10.1016/B978-0-323-91149-8.00009-0.
10. Thakur N, Thakur N, Kumar K, Arya V, Kumar A. Encapsulation of Tinospora cordifolia plant in Ni doped TiO2 nanoparticles for the degradation of malachite green dye. Nanofabrication. 2023. https://doi.org/10.37819/nanofab.8.305.
11. Jha AK, Prasad K, Kulkarni AR. Synthesis of TiO2 nanoparticles using microorganisms. Colloids Surfaces B Biointerfaces. 2009;71(2):226–9. https://doi.org/10.1016/j.colsurfb.2009.02.007.
12. Yaraki MT, Zahed Nasab S, Zare I, Dahri M, Moein Sadeghi M, Koohi M, Tan YN. Biomimetic metallic nanostructures for biomedical applications, catalysis, and beyond. Indus Eng Chem Res. 2022;61(22):7547–93. https://doi.org/10.1021/acs.iecr.2c00285.
13. Jain M, Kapadia R, Jadeja RN, Thounaojam MC, Devkar RV and Mishra SH. Traditional uses, phytochemistry and pharmacology of Tecomellaundulata–A review. Asian Pacific Journal of Tropical Biomedicine. 2012; 2 Issue: 3. S1918-S1923.https://doi.org/10.1016/S2221-1691(12)60521-8
14. Umaralikhan L, Jaffar MJM. Green synthesis of ZnO and Mg doped ZnO nanoparticles, and its optical properties. J Mater Sci Mater Electron. 2017;28:7677–85. https://doi.org/10.1007/s10854-017-6461-1.
15. Ijaz M, Zafar M, Islam A, et al. A review on antibacterial properties of biologically synthesized zinc oxide nanostructures. J Inorg Organomet Polym. 2020;30:2815–26. https://doi.org/10.1007/s10904-020-01603-9.
16. Khanuja M, Uma Varma A. Synthesis and Characterization of Pure and Doped ZnO Nanostructures for Antimicrobial Applications: Effect of Dopant Concentration with Their Mechanism of Action. In: Ghorbanpour, M., Manika, K., Varma, A. (eds) Nanoscience and Plant–Soil Systems. Soil Biology, vol 48. Springer, Cham. 2017; https://doi.org/10.1007/978-3-319-46835-8_6
17. Thakur N, Kumar A, Thakur N. Tinospora cordifolia and polyvinylpyrrolidone encapsulated dual doped Ni-Cu TiO2 emerging nanocatalyst for the removal of organic dyes from wastewater and its free radical assay activity. Hybrid Adv. 2023;4: 100086. https://doi.org/10.1016/j.hybadv.2023.100086.

18. Kumar P, Thakur N, Tapwal A, Kumar S. Enhancing the adsorption capacity of green/chemical synthesized hematite nanoparticles by copper doping: removal of toxic Congo red dye and antioxidant activity. Appl Nanosci. 2023;13(9):6591–604. https://doi.org/10.1007/s13204-023-02943-x.
19. Jiang J, Pi J, Cai J. The advancing of zinc oxide nanoparticles for biomedical applications. Bioinorg Chem Appl. 2018;2018:1–18. https://doi.org/10.1155/2018/1062562.
20. El-Fallal AA, Elfayoumy RA, El-Zahed MM. Antibacterial activity of biosynthesized zinc oxide nanoparticles using Kombucha extract. SN Appl Sci. 2023;5:332. https://doi.org/10.1007/s42452-023-05546-x.
21. Sirelkhatim A, Mahmud S, Seeni A, Kaus NHM, Ann LC, Bakhori SKM, Mohamad D. Review on zinc oxide nanoparticles: antibacterial activity and toxicity mechanism. Nano-micro Lett. 2015;7:219–42. https://doi.org/10.1007/s40820-015-0040-x.
22. Ajitha B. Reddy, Y.A.K. Reddy, P.S. Jeon, H.J. and Ahn C.W.(2016). Role of capping agents in controlling silver nanoparticles size, antibacterial activity and potential application as optical hydrogen peroxide sensor. RSC advances. 6(42): 36171–36179. https://doi.org/10.1039/C6RA03766F
23. Tari O, Aronne A, Addonizio ML, Daliento S, Fanelli E, Pernice P. Sol–gel synthesis of ZnO transparent and conductive films: a critical approach. Solar Energ Mater Solar Cells. 2012;105:179–86. https://doi.org/10.1016/j.solmat.2012.06.016.
24. Cao W, Zhang Y, Wang X, Li Q, Xiao Y, Li P, Xing X. Novel resin-based dental material with anti-biofilm activity and improved mechanical property by incorporating hydrophilic cationic copolymer functionalized nano-diamond. J Mater Sci Mater Med. 2018;29(10):1–13. https://doi.org/10.1007/s10856-018-6172-z.
25. Bala N, Saha S, Chakraborty M, Maiti M, Das S, Basu R, Nandy P. Green synthesis of zinc oxide nanoparticles using Hibiscus subdariffa leaf extract: effect of temperature on synthesis, anti-bacterial activity and anti-diabetic activity. RSC Adv. 2015;7(5):4993–5003. https://doi.org/10.1039/C4RA12784F.
26. Verma R, Dwivedi GK, Singh JP, Singh AP, Tamta N, Kumar A. Characterization of synthesized zinc oxide nanoparticles and their effect on growth, productivity and zinc use efficiency of wheat and field pea in the Indian Himalayan foothills. Curr Sci. 2023. https://doi.org/10.18520/cs/v124/i11/1319-1328.
27. Mishra SK, Srivastava RK, Prakash SG. ZnO nanoparticles: Structural, optical and photoconductivity characteristics. J Alloys Compounds. 2012;539:1–6. https://doi.org/10.1016/j.jallcom.2012.06.024.
28. Jha AK, Prasad K, Prasad K, Kulkarni AR. Plant system: nature's nanofactory. Colloids Surf B. 2009;73(2):219–23. https://doi.org/10.1016/j.colsurfb.2009.05.018.
29. Pantidos N, Horsfall LE. Biological synthesis of metallic nanoparticles by bacteria, fungi and plants. J Nanomed Nanotechnol. 2014;5(5):1. https://doi.org/10.4172/2157-7439.1000233.
30. Mittal AK, Chisti Y, Banerjee UC. Synthesis of metallic nanoparticles using plant extracts. Biotechnol Adv. 2013;31(2):346–56. https://doi.org/10.1016/j.biotechadv.2013.01.003.
31. Sangeetha G, Rajeshwari S, Venckatesh R. Green synthesis of zinc oxide nanoparticles by aloe barbadensis miller leaf extract: structure and optical properties. Mater Res Bull. 2011;46(12):2560–6. https://doi.org/10.1016/j.materresbull.2011.07.046.
32. Chemingui H, Moulahi A, Missaoui T, Al-Marri AH, Hafiane A. A novel green preparation of zinc oxide nanoparticles with Hibiscus sabdariffa L.: photocatalytic performance, evaluation of antioxidant and antibacterial activity. Environ Technol. 2024;45(5):926–44. https://doi.org/10.1080/09593330.2022.2130108.
33. Naiel B, Fawzy M, Halmy MWA, Mahmoud AED. Green synthesis of zinc oxide nanoparticles using Sea Lavender (Limonium pruinosum L. Chaz) extract: characterization, evaluation of anti-skin cancer, antimicrobial and antioxidant potentials. Sci Rep. 2022;12(1):20370. https://doi.org/10.1038/s41598-022-24805-2.
34. Chemingui H, Missaoui T, Mzali JC, Yildiz T, Konyar M, Smiri M, Yatmaz HC. Facile green synthesis of zinc oxide nanoparticles (ZnO NPs): antibacterial and photocatalytic activities. Mater Res Express. 2019;6(10):10504. https://doi.org/10.1088/2053-1591/ab3cd6.
35. Yang Z, Xie C. Zn2+ release from zinc and zinc oxide particles in simulated uterine solution. Colloids Surf B Biointerfaces. 2006;47(2):140–5. https://doi.org/10.1016/j.colsurfb.2005.12.007.
36. Datta A, Patra C, Bharadwaj H, Kaur S, Dimri N, Khajuria R. Green synthesis of zinc oxide nanoparticles using parthenium hysterophorus leaf extract and evaluation of their antibacterial properties. J Biotechnol Biomater. 2017;7(3):271–6. https://doi.org/10.4172/2155-952X.100027.
37. Karam ST, Abdulrahman AF. Green synthesis and characterization of ZnO nanoparticles by using thyme plant leaf extract. Photonics. 2022. https://doi.org/10.3390/photonics9080594.
38. Ramesh M, Anbuvannan M, Viruthagiri GJSAPAM. Green synthesis of ZnO nanoparticles using Solanum nigrum leaf extract and their antibacterial activity. Spectrochim Acta Part A Mol Biomol Spectr. 2015;136:864–70. https://doi.org/10.1016/j.saa.2014.09.105.
39. Upadhyaya H, Shome S, Sarma R, Tewari S, Bhattacharya MK, Panda SK. Green synthesis, characterization and antibacterial activity of ZnO nanoparticles. Am J Plant Sci. 2018;9(6):1279–91. https://doi.org/10.4236/ajps.2018.96094.
40. Sadiq H, Sher F, Sehar S, Lima EC, Zhang S, Iqbal HM, Nuhanović M. Green synthesis of ZnO nanoparticles from SyzygiumCumini leaves extract with robust photocatalysis applications. J Mol Liquids. 2021;335:116567. https://doi.org/10.1016/j.molliq.2021.116567.
41. Thema FT, Manikandan E, Dhlamini MS, Maaza MJML. Green synthesis of ZnO nanoparticles via Agathosmabetulina natural extract. Mater Lett. 2015;161:124–7. https://doi.org/10.1016/j.matlet.2015.08.052.
42. Butnariu M, Coradini CZ. Evaluation of biologically active compounds from *Calendula officinalis* flowers using spectrophotometry. Chem Central J. 2012;6:1–7. https://doi.org/10.1186/1752-153X-6-35.
43. Perveen R, Shujaat S, Qureshi Z, Nawaz S, Khan MI, Iqbal M. Green versus sol-gel synthesis of ZnO nanoparticles and antimicrobial activity evaluation against panel of pathogens. J Mater Res Technol. 2020;9(4):7817–27. https://doi.org/10.1016/j.jmrt.2020.05.004.
44. Wood M. The book of herbal wisdom: using plants as medicines. North AtlantiBooks. 2017. https://www.google.co.in/books/edition/The_Book_of_Herbal_Wisdom/Czw-DwAAQBAJ?hl=en&gbpv=0
45. Medina EJ, Angel LG, Paco L, Algarra I, Collado A, Garrido F. A new extract of the plant *Calendula officinalis* produces a dual in vitro effect. Cytotoxic anti-tumor activity and lymphocyte activation. BMC Cancer. 2006;6:1–4. https://doi.org/10.1186/1471-2407-6-119.
46. Shahen MZ, Mahmud S, Rony MH, Sohana SN, Imran MAS, Al Maruf MA, Alam MS. Effect of antibiotic susceptibility and inhibitory activity for the control of growth and survival of microorganisms of extracts of Calendula officinalis. Eur J Med Health Sci. 2019;1(1):1–9.

47. Tiwari AK, Jha S, Agrawal R, Mishra SK, Pathak AK, Singh AK, Awasthi RR. Anti-bacterial efficacy of phyto-synthesized zinc oxide nanoparticles using Murraya paniculata l. leaf extract. Sciences. 2022;13(4):864–71.
48. Jayachandran A, Aswathy TR, Nair AS. Green synthesis and characterization of zinc oxide nanoparticles using Cayratiapedata leaf extract. Biochem Biophys Rep. 2021;26: 100995. https://doi.org/10.1016/j.bbrep.2021.100995.
49. Kumar MP, Suresh D, Nagabhushana H, Sharma SC. Beta vulgaris aided green synthesis of ZnO nanoparticles and their luminescence, photocatalytic and antioxidant properties. Eur Phys J Plus. 2015;130(6):109. https://doi.org/10.1140/epjp/i2015-15109-2.
50. Tripathi SK, Jha S, Dikshit A, Kumar R. Phytochemical and antioxidant assay of Ecliptaalba (L.) leaf extract. Int J Pharm Sci Res. 2021;12(4):2288–95.
51. Benmehdi H, Behilil A, Memmou F, Amrouche A. Free radical scavenging activity, kinetic behaviour and phytochemical constituents of Aristolochiaclematitis L. roots. Arab J Chem. 2017;10:S1402–8. https://doi.org/10.1016/j.arabjc.2013.04.015.
52. Mydeen SS, Kumar RR, Kottaisamy M, Vasantha VS. Biosynthesis of ZnO nanoparticles through extract from Prosopis juliflora plant leaf: Antibacterial activities and a new approach by rust-induced photocatalysis. J Saudi Chem Soc. 2020;24(5):393–406. https://doi.org/10.1016/j.jscs.2020.03.003.
53. Muniz FTL, Miranda MR, Morilla dos Santos C, Sasaki JM. The Scherrer equation and the dynamical theory of X-ray diffraction. Acta Crystallographica Sec A Foundation Adv. 2016;72(3):385–90. https://doi.org/10.1107/S205327331600365X.
54. Jha S, Singh R, Tiwari AK, Tripathi SK, Pandey A, Dikshit A. Microbial and physic-chemical analysis of palatable water samples from different localities of Prayagraj district. Biochem Cell Arch. 2021;21(2):5149–59.
55. Peng X, Palma S, Fisher NS, Wong SS. Effect of morphology of ZnO nanostructures on their toxicity to marine algae. Aquat Toxicol. 2011;102(3–4):186–96. https://doi.org/10.1016/j.aquatox.2011.01.014.
56. Rad SS, Sani AM, Mohseni S. Biosynthesis, characterization and antimicrobial activities of zinc oxide nanoparticles from leaf extract of Mentha pulegium (L.). Microb Pathog. 2019;131:239–45. https://doi.org/10.1016/j.micpath.2019.04.022.
57. Narendra Kumar HK, Chandra Mohana N, Nuthan BR, Ramesha KP, Rakshith D, Geetha N, Satish S. Phyto-mediated synthesis of zinc oxide nanoparticles using aqueous plant extract of Ocimum americanum and evaluation of its bioactivity. SN Appl Sci. 2019;1:1–9. https://doi.org/10.1007/s42452-019-0671-5.
58. Sasani Ghamsari M, Alamdari S, Han W, Park HH. Impact of nanostructured thin ZnO film in ultraviolet protection. Int J Nanomed. 2017. https://doi.org/10.2147/IJN.S118637.
59. Babayevska N, Przysiecka Ł, Iatsunskyi I, Nowaczyk G, Jarek M, Janiszewska E, Jurga S. ZnO size and shape effect on antibacterial activity and cytotoxicity profile. Sci Rep. 2022;12(1):8148. https://doi.org/10.1038/s41598-022-12134-3.
60. Nayagam V, Gabriel M, Palanisamy K. Green synthesis of silver nanoparticles mediated by Coccinia grandis and Phyllanthus emblica: a comparative comprehension. Appl Nanosci. 2018;8:205–19. https://doi.org/10.1007/s13204-018-0739-3.
61. Pai S, Sridevi H, Varadavenkatesan T, Vinayagam R, Selvaraj R. Photocatalytic zinc oxide nanoparticles synthesis using Peltophorumpterocarpum leaf extract and their characterization. Optik. 2019;185:248–55. https://doi.org/10.1016/j.ijleo.2019.03.101.
62. Tan ST, Chen BJ, Sun XW, Fan WJ, Kwok HS, Zhang XH, Chua SJ. Blueshift of optical band gap in ZnO thin films grown by metal-organic chemicalvapor deposition. J Appl Phys. 2005. https://doi.org/10.1016/j.ijleo.2019.03.101.
63. Thakur N, Thakur N. Removal of organic dyes and free radical assay by encapsulating polyvinylpyrrolidone and Tinospora Cordifolia in dual (Co–Cu) doped TiO2 nanoparticles. Environ Pollut. 2023;335: 122229. https://doi.org/10.1016/j.envpol.2023.122229.
64. Kumar P, Thakur N, Tapwal A, et al. Enhancing the adsorption capacity of green/chemical synthesized hematite nanoparticles by copper doping: removal of toxic Congo red dye and antioxidant activity. Appl Nanosci. 2023;13:6591–604. https://doi.org/10.1007/s13204-023-02943-x.
65. Kumar P, Kumar S, Thakur N. Azadirachta indica and polyvinylpyrrolidone encapsulated Fe2O3 nanoparticles to enhance the photocatalytic and antioxidant activity. Inorg Chem Commun. 2023;155:111084. https://doi.org/10.1016/j.inoche.2023.111084.
66. Kumar P, Kumar S, Tapwal A, et al. Chemical/green synthesized cobalt/copper-doped α-Fe2O3 nanoparticles: potential for environmental remediation. J Mater Res. 2024;39:836–49. https://doi.org/10.1557/s43578-023-01274-5.
67. Debanath MK, Karmakar S. Study of blueshift of optical band gap in zinc oxide (ZnO) nanoparticles prepared by low-temperature wet chemical method. Mater Lett. 2013;111:116–9. https://doi.org/10.1016/j.matlet.2013.08.069.
68. Yakimovich NO, Ezhevskii AA, Guseinov DV, Smirnova LA, Gracheva TA, Klychkov KS. Antioxidant properties of gold nanoparticles studied by ESR spectroscopy. Russian Chem Bullet. 2008;57:520–3. https://doi.org/10.1007/s11172-008-0080-1.
69. Stan M, Popa A, Toloman D, Silipas TD, Vodnar DC. Antibacterial and antioxidant activities of ZnO nanoparticles synthesized using extracts of Allium sativum, Rosmarinus officinalis and Ocimumbasilicum. Acta Metallurgica Sinica. 2016;29:228–36. https://doi.org/10.1007/s40195-016-0380-7.
70. Hossain TJ. Methods for screening and evaluation of antimicrobial activity: a review of protocols, advantages and limitations. Adv Limitations (July 17, 2023).
71. MuthuKathija M, Badhusha MSM, Rama V. Green synthesis of zinc oxide nanoparticles using Pisonia Alba leaf extract and its antibacterial activity. Appl Surf Sci Adv. 2023;15: 100400. https://doi.org/10.1016/j.apsadv.2023.100400.
72. Gudkov SV, Burmistrov DE, Serov DA, Rebezov MB, Semenova AA, Lisitsyn AB. A mini review of antibacterial properties of ZnO nanoparticles. Front Phys. 2021;9: 641481.
73. Sirelkhatim A, Mahmud S, Seeni A, Kaus NHM, Ann LC, Bakhori SKM, Mohamad D. Review on zinc oxide nanoparticles: antibacterial activity and toxicity mechanism. Nano-micro Lett. 2015;7:219–42.
74. Steffy K, Shanthi G, Maroky AS, Selvakumar S. Synthesis and characterization of ZnOphytonanocomposite using Strychnos nux-vomica L. (Loganiaceae) and antimicrobial activity against multidrug-resistant bacterial strains from diabetic foot ulcer. J Adv Res. 2018;9:69–77. https://doi.org/10.1016/j.jare.2017.11.001.
75. Mahendra C, Chandra MN, Murali M, Abhilash MR, Singh SB, Satish S, Sudarshana MS. Phyto-fabricated ZnO nanoparticles from Canthiumdicoccum (L.) for antimicrobial, anti-tuberculosis and antioxidant activity. Process Biochem. 2020;89:220–6. https://doi.org/10.1016/j.procbio.2019.10.020.

Publisher's Note Springer Nature remains neutral with regard to jurisdictional claims in published maps and institutional affiliations.